

Relaxation and Noise in Chaotic Systems

Shmuel Fishman and Saar Rahav
Department of Physics, Technion, Haifa 32000, Israel
(Date: November 20, 2018)

For a class of idealized chaotic systems (hyperbolic systems) correlations decay exponentially in time. This result is asymptotic and rigorous. The decay rate is related to the Ruelle-Pollicott resonances. Nearly all chaotic model systems, that are studied by physicists, are not hyperbolic. For many such systems it is known that exponential decay takes place for a long time. It may not be asymptotic, but it may persist for a very long time, longer than any time of experimental relevance. In this review a heuristic method for calculation of this exponential decay of correlations in time is presented. It can be applied to model systems, where there are no rigorous results concerning this exponential decay. It was tested for several realistic systems (kicked rotor and kicked top) in addition to idealized systems (baker map and perturbed cat map). The method consists of truncation of the evolution operator (Frobenius-Perron operator), and performing all calculations with the resulting finite dimensional matrix. This finite dimensional approximation can be considered as coarse graining, and is equivalent to the effect of noise. The exponential decay rate of the chaotic system is obtained when the dimensionality of the approximate evolution operator is taken to infinity, resulting in infinitely fine resolution, that is equivalent to vanishing noise. The corresponding Ruelle-Pollicott resonances can be calculated for many systems that are beyond the validity of the Ruelle-Pollicott theorem.

I. INTRODUCTION

The purpose of the lectures that are summarized in this review is to describe the behavior of ensembles of chaotic systems. As in the case of statistical mechanics, the dynamics of ensembles turns out to be simpler than the one of individual systems. For chaotic systems [1–7] the long time asymptotic behavior is rigorously known to exhibit exponential decay of correlations only for a class of idealized systems (hyperbolic systems). Physical model systems do not belong to this class. In what follows *nonrigorous* methods, that enable the exploration of the long time behavior of chaotic systems, are presented and their application is demonstrated for several systems. The review is pedagogical and descriptive in nature, and is intended for an overview of the subject. The reader should consult the references for the details and the precise statements.

The dynamics of the systems considered in this review is of Hamiltonian nature. The dynamics of the continuous systems is determined by the Hamilton equations:

$$\begin{aligned}\dot{p} &= -\frac{\partial \mathcal{H}}{\partial q} \\ \dot{q} &= \frac{\partial \mathcal{H}}{\partial p}\end{aligned}\tag{1}$$

where \mathcal{H} is the Hamiltonian, while q and p are the position and momentum respectively. The phase space density $\rho(\mathbf{x})$, where $\mathbf{x} = (q, p)$ are the phase space points, satisfies the Liouville theorem,

$$\frac{d\rho}{dt} = 0\tag{2}$$

or

$$\frac{\partial \rho}{\partial t} = \{\mathcal{H}, \rho\},\tag{3}$$

where $\{\dots\}$ are the Poisson brackets. The main issue that will be discussed is the way ρ spreads in phase space for chaotic systems. For classical chaotic systems finer and finer structures develop for longer and longer times. These structures are reflected in ρ . Coarse graining, with some fixed scale of resolution, results in the truncation of the evolution of these very fine structures. On the finite (but arbitrarily small) resolution scale the equilibrium uniform phase space density is approached. In this review the asymptotic (in time) relaxation to this density will be discussed and in the end the coarse graining scale will be taken to 0. The results differ from the ones obtained without coarse graining, since the limits of infinite time and vanishing coarse graining do not commute. The approach, where a finite resolution scale is used and then the limit where this scale tends to zero is taken, is relevant for experimental

realizations where the idealized classical description on the finest scales is destroyed resulting of the coupling to the environment.

Maps are transformations of phase space in discrete time, denoted by n . A map \mathbf{F} is a transformation

$$\mathbf{x}_{n+1} = \mathbf{F}(\mathbf{x}_n). \quad (4)$$

We study maps since they are easier to handle analytically and numerically and they reproduce the most interesting results found for systems evolving continuously in time.

Maps can be derived from Hamiltonians of the form:

$$\mathcal{H} = \frac{p^2}{2} + V(q) \sum_n \delta(t - n). \quad (5)$$

For such maps the phase space area is preserved. Maps can also be defined with no reference to a Hamiltonian. The dynamics of phase space densities will be explored here for several area preserving maps: a. Kicked Rotor (Standard Map), b. Kicked Top, c. Arnold Cat Map and d. Baker Map.

a. Kicked Rotor (Standard Map)

A planar rotor that is periodically kicked is modeled by the Hamiltonian [1,3,7]

$$\mathcal{H} = \frac{J^2}{2} + K \cos \theta \sum_n \delta(t - n), \quad (6)$$

where θ is the coordinate and J is the conjugate momentum. The Hamilton equations (1) are:

$$\begin{aligned} \dot{\theta} &= J \\ \dot{J} &= K \sin \theta \sum_n \delta(t - n). \end{aligned} \quad (7)$$

Integration with respect to time results in the Standard Map

$$\begin{aligned} \theta_{n+1} &= \theta_n + J_n \\ J_{n+1} &= J_n + K \sin \theta_{n+1}, \end{aligned} \quad (8)$$

where θ_n and J_n are the angle and angular momentum just after the n -th kick. The equations (8) define a map of the form (4)

$$(\theta_{n+1}, J_{n+1}) = \mathbf{F}(\theta_n, J_n). \quad (9)$$

It is easily checked that the map is area preserving. It becomes more chaotic as the stochasticity parameter K increases. The phase space is plotted in Fig. 1.

A variant of this map provides a good description of driven laser cooled atoms [8] and of beams deflected by dielectrics with a modulated index of refraction [9].

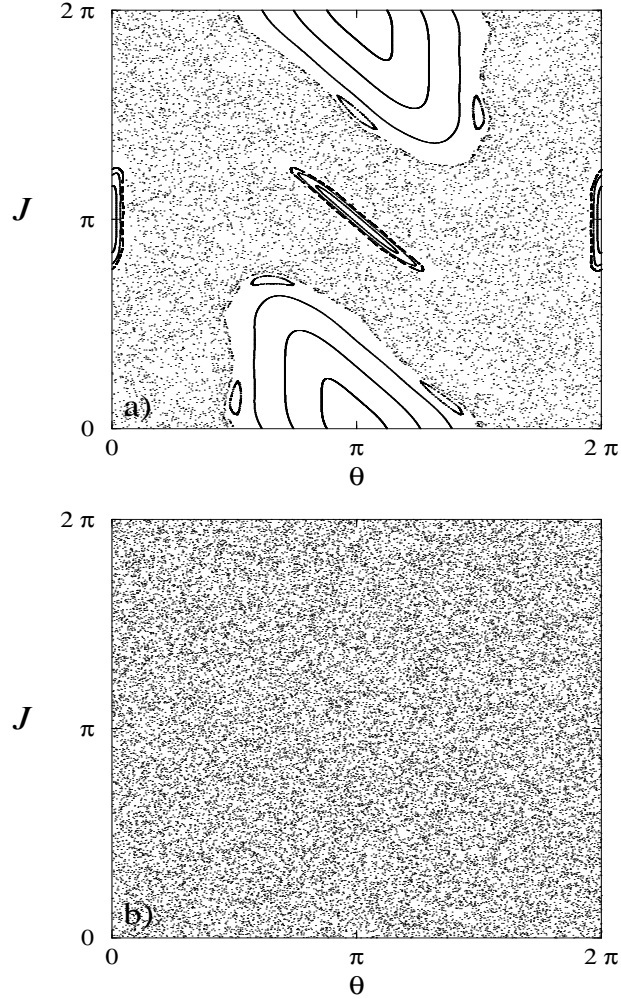


FIG. 1. Phase space portraits of the weakly chaotic kicked rotor with stochasticity parameter $K = 2$ (a), and of the strongly chaotic kicked rotor with $K = 10$ (b).

b. Kicked Top

A large spin can be described by a classical vector

$$\mathbf{J} = j (\sin \theta \cos \varphi, \sin \theta \sin \varphi, \cos \theta) \quad (10)$$

where θ and φ are the polar angles. The kicked top map is defined by the transformation [3]

$$\mathbf{F} = R_z(\tau \cos \theta) R_z(\beta_z) R_y(\beta_y), \quad (11)$$

applied to \mathbf{J} where $R_i(\beta)$ is the rotation around the axis i by the angle β . The nonlinearity results of the dependence of a rotation on the angle θ . The chaoticity of the map increases with τ that is the stochasticity parameter. The canonical phase space variables for this map are $q = \varphi$ and $p = \cos \theta$. The phase space is plotted in Fig. 2.

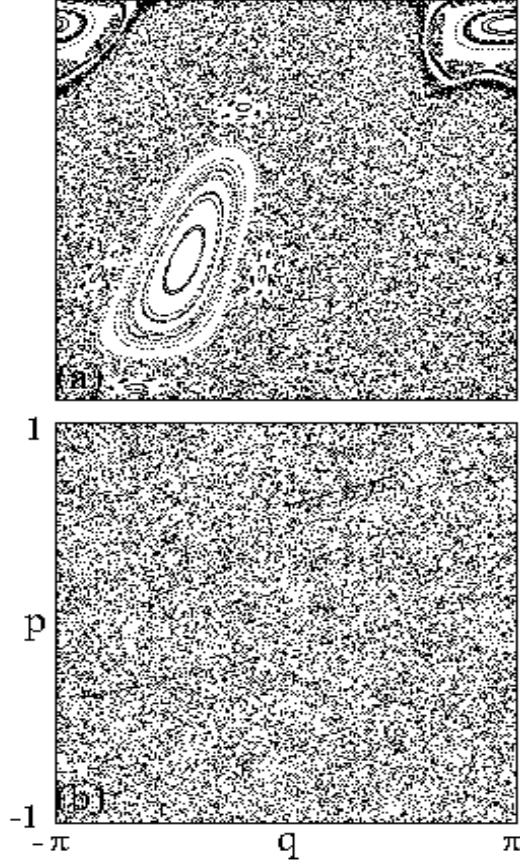


FIG. 2. Phase space portraits of the weakly chaotic kicked top with stochasticity parameter $\tau = 2.1$ (a), and of the strongly chaotic kicked top with $\tau = 10.2$ (b). (Fig. 1 of [10]).

c. Arnold Cat Map

It is defined in the $[0, 1] \times [0, 1]$ square of the (x, y) phase plane by [2,4]

$$\begin{aligned} x_{n+1} &= x_n + y_n \quad \text{mod } 1 \\ y_{n+1} &= x_n + 2y_n \quad \text{mod } 1. \end{aligned} \tag{12}$$

The evolution is demonstrated in [2,4].

d. Baker map

It is defined in the $[0, 1] \times [0, 1]$ square of the (x, y) phase plane by [4,6,1]

$$(x_{n+1}, y_{n+1}) = \mathbf{F}(x_n, y_n) = \begin{cases} (2x_n, y_n/2) & \text{for } 0 \leq x < \frac{1}{2} \\ (2x_n - 1, (y_n + 1)/2) & \text{for } \frac{1}{2} \leq x < 1 \end{cases} \tag{13}$$

This transformation is demonstrated in Fig. 3.

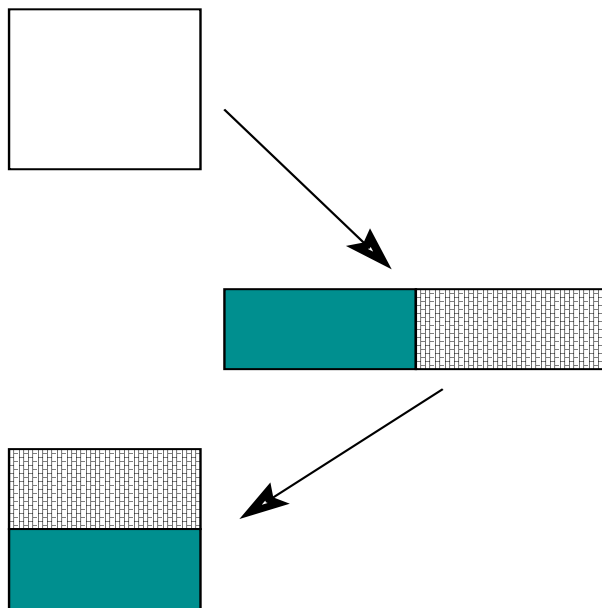


FIG. 3. The baker map.

The systems (a) and (b) model physical problems. Their phase space is mixed, namely the dynamics in some parts is chaotic and in some parts it is regular. Systems (c) and (d) are very idealized. For these systems the motion is chaotic in the entire phase space.

A system is chaotic if points, that are initially close, spread exponentially in phase space. For chaotic systems the separation between points grows with the number of steps as

$$\epsilon(n) = \epsilon(0)\Lambda^n, \quad (14)$$

in the limit $n \rightarrow \infty$ and $\epsilon(0) \rightarrow 0$. The Lyapunov exponent is

$$\lambda = \ln \Lambda \quad (15)$$

and Λ is sometimes called the Lyapunov number. A system that evolves in a bounded region in phase space is called *chaotic* if its Lyapunov exponent λ according to the definition (14,15) is positive. (More generally the Lyapunov numbers are the eigenvalues of the tangent map. The Lyapunov number defined by (14) is equal to the magnitude of the largest eigenvalue.) One can study the local expansion and contraction in the various directions. If for a map, for any point of phase space, in each direction, either expansion or contraction takes place, or in other words if none of the real parts of the local Lyapunov exponents vanishes, the system is called *hyperbolic*.

Exponential spread of trajectories in phase space does *not* imply exponential decay of correlations in time. Such correlations may result of sticking to small structures in phase space, as is the case for the stadium billiard and for the Sinai billiard as well as for chaotic trajectories of mixed systems, such as the kicked rotor and the kicked top. For hyperbolic systems, such as the baker map, typically correlations in time decay exponentially.

Chaotic motion is reminiscent of a random walk. Therefore it is instructive to review the dynamics of the probability density of random walkers. Assume a random walk on a one dimensional lattice, with equal probability of 1/2 to make a step to the left or to the right. The path of each walker is complicated but the evolution of a probability density of random walkers is simple. It is simple in particular in the continuum approximation (the limit of vanishing lattice spacing) where it is described by the diffusion equation

$$\frac{\partial}{\partial t} \rho(x, t) = D \frac{\partial^2}{\partial x^2} \rho(x, t), \quad (16)$$

D is the diffusion coefficient and $\rho(x, t)$ is the density of random walkers at the point x at time t . Let us assume that the random walk is confined to an interval of length s , for example $-s/2 < x < s/2$. The current at the ends of the interval vanishes, resulting in the boundary conditions

$$\frac{\partial \rho}{\partial x} \Big|_{x=\pm s/2} = 0 \quad (17)$$

on (16). This problem is similar to the standard quantum mechanical problem of a particle in an infinite square well, but with the boundary conditions (17) and with no $i\hbar$ on the left hand side of (16). Therefore the density of states can be expanded as:

$$\rho(x, t) = \sum_{k=0}^{\infty} a_k e^{-\gamma_k t} u_k(x), \quad (18)$$

where

$$u_k = \begin{cases} \sqrt{\frac{2}{s}} \left[\cos \frac{\pi x}{s} k + \left(\sqrt{\frac{1}{2}} - 1 \right) \delta_{k0} \right] & k \text{ even} \\ \sqrt{\frac{2}{s}} \sin \frac{\pi x}{s} k & k \text{ odd} \end{cases} \quad (19)$$

form an orthonormal basis and

$$\gamma_k = \left(\frac{\pi k}{s} \right)^2 D. \quad (20)$$

The units of a_k are of $1/\sqrt{[\text{length}]}$. The expansion coefficients a_k are determined by the initial density $\rho(x, t = 0)$. The equilibrium density is

$$\lim_{t \rightarrow \infty} \rho(x, t) = a_0 \sqrt{\frac{1}{s}}, \quad (21)$$

and the asymptotic approach to this density is

$$\rho(x, t) - \frac{a_0}{\sqrt{s}} \sim a_1 e^{-\gamma_1 t} u_1(x) \quad (22)$$

with the relaxation rate $\gamma_1 = \left(\frac{\pi}{s} \right)^2 D$. The density-density correlation function is

$$C(t) = \int_{-s/2}^{s/2} dx \rho(x, 0) \rho(x, t) - a_0^2 = \sum_{k=1}^{\infty} |a_k|^2 e^{-\gamma_k t} \sim |a_1|^2 e^{-\gamma_1 t}. \quad (23)$$

Hence also the correlations decay with the rate γ_1 .

The example of the probability density of random walkers demonstrates that although the trajectories of specific random walkers are complicated their probability density ρ follows simple dynamics. We turn now to study the phase space probability density $\rho(\mathbf{x})$, that for Hamiltonian dynamics satisfies (3). The introduction of such probability densities, that are sufficiently smooth, is actually a coarse graining over some fine scale. It is an averaging over phase space of the same type that was performed for random walkers. For any given area preserving map \mathbf{F} it is instructive to introduce the one step evolution operator \hat{U} ,

$$\rho_{n+1}(\mathbf{x}) = \hat{U} \rho_n(\mathbf{x}), \quad (24)$$

where $\rho_n(\mathbf{x})$ is the phase space density after n steps of the map. If the operator is defined on a space of sufficiently smooth functions it is called the *Frobenius-Perron operator*. If \mathbf{F} is area preserving and invertible, namely if \mathbf{F}^{-1} exists, then \hat{U} is unitary. All eigenvalues of \hat{U} are on the unit circle in the complex plane, they take the form $e^{-i2\pi\alpha}$, with real α . The corresponding ‘‘eigenfunctions’’ are not square integrable. An example of such a function will be presented now [11]. Assume the map \mathbf{F} has a periodic orbit of period n , that is:

$$\begin{aligned} \mathbf{x}_{j+1} &= \mathbf{F}(\mathbf{x}_j), & j &= 1, 2, \dots, n \\ \mathbf{x}_1 &= \mathbf{F}(\mathbf{x}_n). \end{aligned} \quad (25)$$

The function

$$\psi_\alpha(\mathbf{x}) = \sum_{j=1}^n \delta(\mathbf{x} - \mathbf{x}_j) e^{i2\pi\alpha j} \quad (26)$$

with $\alpha = l/n$, where l is an integer, is an “eigenfunction” of \hat{U} with the eigenvalue $e^{-i2\pi\alpha}$. Here ψ_α is called “eigenfunction” if

$$\hat{U}\psi_\alpha = e^{-i2\pi\alpha}\psi_\alpha \quad (27)$$

and no requirement is made that it belongs to the space where \hat{U} is defined. For example if \hat{U} is defined on the space of square integrable functions, ψ_α of (26) does not belong to this space and is not a function in the usual sense (it is a distribution).

The operator \hat{U} can be represented by an infinite dimensional matrix. In physics applications it is natural to use finite dimensional approximations. Let us assume that a basis that is ordered by increased resolution is used (the basis states may be for example sines and cosines or orthogonal polynomials). For the truncation of \hat{U} , namely a finite dimensional approximation, the matrix is not unitary, and its eigenvalues are inside the unit circle in the complex plane. They may vary with the dimension of the matrix. The natural question is: Do these eigenvalues approach the unit circle in the limit of an infinite dimensional matrix? It will be demonstrated in what follows that this is *not* the case for chaotic systems and values *inside* the unit circle are approached in this limit, in spite of the fact that the infinite dimensional matrix representing \hat{U} is unitary. A heuristic justification for this behavior was proposed by F. Haake [10]. Chaotic systems, in contrast with regular ones, exhibit phase space structures on all scales. These structures are revealed during the evolution. The operator \hat{U} couples the fine scales via its matrix elements that couple to states with high resolution. As a result of the truncation, probability that was originally transferred to the fine scales is lost, resulting in nonunitarity of \hat{U} . Convergence of the eigenvalues to values inside the unit circle in the complex plane, in the limit of infinite dimension of the matrix, results of the asymptotic self similarity of the chaotic dynamics. For regular motion, on the other hand, as the dimension of the matrix is increased the eigenvalues approach the unit circle [10] (see Sec. IV).

It will be shown that for chaotic systems the finite dimensional approximations of \hat{U} , in the limit of large dimension, describe the decay of correlations. The phase space density-density correlation function, in analogy with (23) is

$$\begin{aligned} C(n) &= \int d\mathbf{x} \rho(\mathbf{x}, 0) \rho(\mathbf{x}, n) - \rho_\infty^2 \Omega \\ &= \int d\mathbf{x} \rho(\mathbf{x}, 0) \hat{U}^n \rho(\mathbf{x}, 0) - \rho_\infty^2 \Omega, \end{aligned} \quad (28)$$

where Ω is the volume of the chaotic component in phase space. The equilibrium density is $\rho_\infty = \lim_{n \rightarrow \infty} \rho(\mathbf{x}, n)$ that is independent of position in phase space. A more general correlation function is:

$$C^{(A,B)}(n) = \int d\mathbf{x} A(\mathbf{x}) \hat{U}^n B(\mathbf{x}), \quad (29)$$

where we assumed

$$\lim_{n \rightarrow \infty} \hat{U}^n A(\mathbf{x}) = \lim_{n \rightarrow \infty} \hat{U}^n B(\mathbf{x}) = 0. \quad (30)$$

This can always be obtained by the subtraction of the asymptotic value. For simplicity it will be assumed that both A and B are real.

It is useful to study the Laplace transforms of the correlation functions. For this purpose we introduce the resolvent

$$\hat{R}(z) = \frac{1}{z} \sum_{j=0}^{\infty} \hat{U}^j z^{-j} = \frac{1}{z - \hat{U}} \quad (31)$$

where z is a complex number. Since \hat{U} is unitary the sum is convergent for $|z| > 1$. This is analogous to the usual definition used in quantum mechanics:

$$\hat{R}(E) = \frac{1}{i\hbar} \int_0^{\infty} dt \hat{U} \exp\left(\frac{i}{\hbar} Et - \frac{\epsilon}{\hbar} t\right), \quad (32)$$

where

$$\hat{U} = \exp\left(-\frac{i}{\hbar} \hat{H} t\right) \quad (33)$$

is the evolution operator, leading to

$$\hat{R}(E) = \frac{1}{E - \hat{\mathcal{H}} + i\epsilon} \quad (34)$$

for $\epsilon > 0$. The convergence of the integral (32) requires $\epsilon > 0$. In analogy the convergence of the sum (31) requires $|z| > 1$ in (31). The discrete Laplace (one sided Fourier) transform of the correlation function (29) is

$$\tilde{C}^{(A,B)}(z) = \sum_{n=0}^{\infty} C^{(A,B)}(n)z^{-n} = \int d\mathbf{x} A(\mathbf{x}) \left[z\hat{R}(z) \right] B(\mathbf{x}), \quad (35)$$

as one finds from (31).

Let ψ_i be an ‘‘eigenfunction’’ of \hat{U} with the eigenvalue z_i ,

$$\hat{U}\psi_i = z_i\psi_i. \quad (36)$$

By ‘‘eigenfunction’’ we mean here that it satisfies (36), but it may not be a function in the usual sense (for example it may be a distribution). Then z_i is a pole of the matrix elements of the resolvent as one can see from (31). The correlation function, involving an ‘‘eigenfunction’’, takes the form

$$\tilde{C}^{(A,\psi_i)}(z) = \langle A|\psi_i \rangle \frac{z}{z - z_i}, \quad (37)$$

where the Dirac notation

$$\langle A|B \rangle = \int d\mathbf{x} A^*(\mathbf{x})B(\mathbf{x}) \quad (38)$$

is used (A^* is the complex conjugate of A). Here A and B were assumed to be real. Let us expand $B(\mathbf{x})$ in terms of the ‘‘eigenfunctions’’ of \hat{U} as

$$B(\mathbf{x}) = \sum_i b_i \psi_i(\mathbf{x}). \quad (39)$$

Then

$$\tilde{C}^{(A,B)}(z) = \frac{r_i}{z - z_i} \quad (40)$$

where the poles z_i depend only on \hat{U} while the residues

$$r_i = b_i \langle A|\psi_i \rangle, \quad (41)$$

depend also on A and B .

Because of the unusual nature of the ‘‘eigenfunctions’’ ψ_i the manipulations leading to (40) are only heuristic. The Ruelle-Pollicott theorem justifies the expression (40) for *hyperbolic* systems if A and B are typical smooth functions (for a precise statement of the theorem that is transparent for physicists see [12]). Moreover the theorem assures that $|z_i| < 1$, except for the eigenvalue $z_0 = 1$ corresponding to the equilibrium density ψ_0 , that is independent of \mathbf{x} . The z_i are called the Ruelle-Pollicott resonances.

The existence of poles with $|z_i| < 1$ implies the decay of correlations with the rate $\ln |z_i|$. This results of

$$C^{(A,B)}(n) = \frac{1}{2\pi i} \oint_{|z|=1} \frac{dz}{z} \tilde{C}^{(A,B)}(z)z^n \quad (42)$$

and the application of the residue theorem to (40).

For any approximation of dimension N of the Frobenius-Perron operator \hat{U} , that will be denoted by $\hat{U}^{(N)}$ in what follows, the eigenfunctions $\psi_i^{(N)}$, corresponding to the eigenvalues $z_i^{(N)}$, are well defined. For hyperbolic systems, where the Ruelle-Pollicott theorem applies, it is reasonable to assume that in the limit $N \rightarrow \infty$, the eigenvalues $z_i^{(N)}$ approach the Ruelle-Pollicott resonances, for a typical choice of the basis. Inspired by the Ruelle-Pollicott theorem the following heuristic scheme for the calculation of the decay rates of correlations is proposed:

1. Introduce an orthogonal basis where the basis states are ordered by resolution. These states, for example, may be orthogonal polynomials or trigonometric functions ($\cos 2\pi kx, \sin 2\pi kx$) or exponentials $\exp i2\pi kx$.
2. Calculate the matrix elements of \hat{U} in this basis.
3. Introduce a truncation of dimension N of this matrix, that will be denoted as $\hat{U}^{(N)}$.
4. Calculate the eigenvalues $z_i^{(N)}$ and the eigenfunctions $\psi_i^{(N)}$ of $\hat{U}^{(N)}$. The eigenfunctions $\psi_i^{(N)}$ are finite linear combinations of the basis states, and therefore are smooth.
5. Take the limit $N \rightarrow \infty$. In this limit $z_i^{(N)} \rightarrow z_i$ and $\psi_i^{(N)} \rightarrow \psi_i$.

From the Ruelle-Pollicott theorem it is expected, for hyperbolic systems, that the Ruelle-Pollicott resonances are obtained in this way, if a typical basis is used. The limiting functions ψ_i are singular [13–15]. This scheme was applied to various systems, including also to mixed systems [10,16–20]. Limiting eigenvalues z_i satisfying $|z_i| < 1$ were obtained in this way, implying exponential relaxation of correlations with the rate $\ln |z_i|$ that takes place for a very long time (for some nonhyperbolic systems it is known that eventually the correlations decay as a power-law, but the time required to obtain this power-law behavior may be too long for any physical relevance). Although the Hamiltonian dynamics of trajectories is reversible the phase space densities exhibit relaxation that is irreversible, and is similar to the behavior of probability densities of random walkers that follow irreversible dynamics.

In Sec. II the heuristic scheme for the calculation of the z_i will be demonstrated for the baker map that is hyperbolic and consequently the Ruelle-Pollicott theorem applies. Exploration of a hyperbolic system that is a modification of the cat map is briefly mentioned in Sec. III. In Sec. IV the scheme will be applied to the kicked top and in Sec. V it will be applied to the kicked rotor, that are mixed systems, where the Ruelle-Pollicott theorem is not valid. Also the limitations on the validity of this scheme for such systems will be demonstrated. The main conclusions are summarized in Sec. VI. The review will follow closely references [10,13,19], that are marked by ** in the list of references. A detailed discussion on the relaxation of correlations in chaotic systems and on related topics can be found in [5,6]. The scheme for the use of truncation in the calculation of the Ruelle-Pollicott resonances is discussed in a wider context in [14].

II. THE FROBENIUS-PERRON OPERATOR FOR THE BAKER MAP, A DEMONSTRATION

The heuristic prescription for the analysis of the Frobenius-Perron operator that was outlined in the Introduction will be demonstrated for the baker map (13), where all the results are exactly known. The analysis will make use of exact results obtained in [13].

The basis states that will be used are

$$\langle xy|kl\rangle = \tilde{P}_k(x)\tilde{P}_l(y) \quad (43)$$

where

$$\tilde{P}_k(x) = \sqrt{2k+1}P_k(1-2x) = \frac{\sqrt{2k+1}}{k!} \frac{d^k}{dx^k} x^k (1-x)^k \quad (44)$$

are the modified Legendre polynomials while P_k are the Legendre polynomials. A basis of orthogonal polynomials is natural, since the order of the polynomial is not affected by the map (13). The orthonormality of the basis

$$\langle kl|k'l'\rangle = \delta_{kk'}\delta_{ll'} \quad (45)$$

follows from the orthonormality of the modified Legendre polynomials

$$\int_0^1 dx \tilde{P}_k(x)\tilde{P}_{k'}(x) = \delta_{kk'}. \quad (46)$$

The basis is naturally ordered by increased resolution, since this is a property of orthogonal polynomials. The action of \hat{U} of (24) on any phase space density is

$$\hat{U}\rho(\mathbf{x}) = \rho(\mathbf{F}^{-1}(\mathbf{x})), \quad (47)$$

since the points that are at \mathbf{x} at time step $n + 1$ were at $\mathbf{F}^{-1}(\mathbf{x})$ the time step n . For the baker map (13)

$$\rho(\mathbf{F}^{-1}(x, y)) = \begin{cases} (\rho(x/2, 2y)) & \text{for } 0 \leq y < \frac{1}{2} \\ (\rho((x+1)/2, 2y-1)) & \text{for } \frac{1}{2} \leq y < 1. \end{cases} \quad (48)$$

From (47) and (48) one finds that the matrix elements of \hat{U} are

$$\langle kl|\hat{U}|k'l'\rangle = \frac{1}{2} \left[1 + (-1)^{k+k'+l+l'} \right] I_{kk'} I_{l'l} \quad (49)$$

where

$$I_{kk'} = \int_0^1 dx \tilde{P}_k(x) \tilde{P}_{k'}(x/2). \quad (50)$$

Using (44) and integrating (50) by parts k times one finds that if $k > k'$,

$$I_{kk'} = 0. \quad (51)$$

This results in the *nonrecurrence* property of \hat{U}

$$\langle kl|\hat{U}|k'l'\rangle = 0 \quad \text{for } k > k' \text{ or } l' > l. \quad (52)$$

During the evolution, probability is transformed from states with k' to states with k only if $k \leq k'$, therefore after application of \hat{U} the density becomes more uniform because the weight of lower order Legendre polynomials is increased. This is expected since x is the unstable direction, where stretching takes place, making the density more uniform. In the y direction, on the other hand, the density is transformed from l' to l only if $l \geq l'$, therefore during the evolution, the weight of the high order Legendre polynomials increases. This results of the fact that y is the stable direction, where contraction takes place, resulting in complexity that increases with time.

For $k \leq k'$ one finds [13]

$$I_{kk'} = \frac{[(2k+1)(2k'+1)]^{1/2}}{2^k} \sum_{l=0}^{k'-k} \left(-\frac{1}{2}\right)^l \frac{(k'+k+l)!}{(k'-k-l)!(2k+l+1)!l!}. \quad (53)$$

In particular $I_{kk} = 2^{-k}$ and the diagonal matrix elements are

$$\langle kl|\hat{U}|kl\rangle = \frac{1}{2^{k+l}}. \quad (54)$$

The matrix elements of \hat{U}^n can be calculated with the help of the nonrecurrence property (52). Introducing the resolution of the identity one finds

$$\langle kl|\hat{U}^n|k'l'\rangle = \sum_{[k_i; l_i]} \langle kl|\hat{U}|k_1 l_1\rangle \langle k_1 l_1|\hat{U}|k_2 l_2\rangle \dots \dots \dots \langle k_{n-1} l_{n-1}|\hat{U}|k' l'\rangle, \quad (55)$$

where $[k_i; l_i] \equiv [k_1, k_2, \dots, k_{n-1}; l_1, l_2, \dots, l_{n-1}]$ and the nonrecurrence property implies $k \leq k_1 \leq k_2, \dots \dots \dots \leq k'$ and $l \geq l_1 \geq l_2, \dots \dots \dots \geq l'$. In particular the diagonal matrix elements satisfy

$$\langle kl|\hat{U}^n|kl\rangle = \langle kl|\hat{U}|kl\rangle^n = \left(\frac{1}{2^{k+l}}\right)^n. \quad (56)$$

In the limit $n \rightarrow \infty$ the off-diagonal matrix elements are dominated by powers of the diagonal matrix elements, since the nonrecurrence property limits the number of non-diagonal matrix elements in (55).

The diagonal matrix elements of the resolvent can be easily calculated with the help of (31). For $|z| > 1$ the sum in (31) is convergent and using (56) one finds

$$\langle kl|\hat{R}(z)|kl\rangle = \sum_{n=0}^{\infty} z^{-(n+1)} \langle kl|\hat{U}|kl\rangle^n = \frac{1}{z - 2^{-(k+l)}}. \quad (57)$$

These matrix elements are singular for $z = 2^{-(k+l)}$, and except for $k = l = 0$ all these singular points are inside the unit circle in the complex plane. This is also the case for the off-diagonal matrix elements. Therefore the Ruelle-Pollicott resonances are

$$z_m = 2^{-m} \quad (58)$$

and their degeneracy is $m + 1$. They are related to the decay of correlations by (40). They were obtained by analytic continuation from $|z| > 1$ where the resolvent is defined. One can show [13] that the matrix elements exhibit a cut at $|z| = 1$ and the physically relevant poles are on the Riemann sheet continued from $|z| > 1$.

What happens if the Frobenius-Perron operator is restricted to $k, k' \leq k_{max}$ and $l, l' \leq l_{max}$ and \hat{U} is approximated by $\hat{U}^{(N)}$, an $N = k_{max}l_{max}$ dimensional matrix, resulting of the truncation of \hat{U} ? The nonrecurrence property holds for $\hat{U}^{(N)}$ and consequently (56) holds. Therefore for the N dimensional matrix $\hat{U}^{(N)}$ the diagonal matrix elements, are zeros of the characteristic polynomial, that is of order N . To see this, note that by the Hamilton-Cayley theorem, $\hat{U}^{(N)}$ satisfies its characteristic polynomial, namely $\sum_{j=0}^N p_j \hat{U}^{(N)j} = 0$, and calculate the diagonal matrix elements of this expression with the help of (56). Consequently the diagonal matrix elements are eigenvalues of $\hat{U}^{(N)}$, taking the values 2^{-m} . The multiplicity of the eigenvalue 2^{-m} is $m + 1$ if $m \leq k_{max}, l_{max}$. By a similarity transformation the matrix can be transformed to the canonical Jordan form. Another way to see that the eigenvalues of $\hat{U}^{(N)}$ coincide with the diagonal matrix elements is by using the indices $l_{max} - l$ and $l_{max} - l'$ instead of l and l' . With these indices, $\hat{U}^{(N)}$ is upper triangular, therefore the eigenvalues coincide with the diagonal matrix elements. The eigenvalues are independent of k_{max} and l_{max} , therefore these are of the form 2^{-m} also in the limit $k_{max} \rightarrow \infty$ and $l_{max} \rightarrow \infty$, in spite of the fact that \hat{U} is unitary. For $\hat{U}^{(N)}$ the eigenfunctions are finite combinations of Legendre polynomials and are therefore smooth. In the limit $k_{max} \rightarrow \infty$ and $l_{max} \rightarrow \infty$ the right eigenfunctions are independent of x and are polynomials of y , while the left eigenfunctions tend to distributions [13].

The main results that were obtained for the baker map are:

1. A basis that is ordered by increased resolution was introduced. A truncation of dimension N in this basis was implemented.
2. The Ruelle-Pollicott resonances were calculated from $\hat{U}^{(N)}$, the N dimensional truncation of \hat{U} . As N increases more eigenvalues are revealed. The values of the eigenvalues do not depend on the truncation dimension N , and therefore also in the limit of infinite N they remain at values that were obtained for finite N .
3. The poles of the matrix elements of the resolvent (31) and (57) were obtained by analytic continuation from $|z| > 1$.
4. The eigenfunctions of \hat{U} are functions of y only (y is the stable direction).

In this section the procedure for the calculation of Ruelle-Pollicott resonances from $\hat{U}^{(N)}$, a truncated matrix approximating \hat{U} , was demonstrated for a system where the results are known exactly. In the following sections this method will be applied to systems where there is no exact theory.

The basis used here was of Legendre polynomials. If a basis of sines and cosines is used it is impossible to find the Ruelle-Pollicott resonances in this way, since each of the basis states collapses to 0 after a finite number of applications of \hat{U} [13,21]. On the basis of the Ruelle-Pollicott theorem, we believe that for a typical basis one does not encounter problems of this nature.

III. THE FROBENIUS-PERRON OPERATOR OF A MODIFIED CAT MAP

For the Arnold cat map, defined by (12), correlations in time decay faster than exponentially. A modification, where the function $f(x_{n+1})$, that is defined by

$$f(x) = \frac{K_0}{2\pi} [\cos(2\pi x) - \cos(4\pi x)], \quad (59)$$

is added to the equation for y_{n+1} in (12), is a hyperbolic system if K_0 is sufficiently small [22]. The correlations for this system decay exponentially in time. It was studied with the help of the truncated Frobenius-Perron operator, according to the scheme that was outlined in the introduction. The leading Ruelle-Pollicott resonances were found with the help of a variational approach.

IV. THE FROBENIUS-PERRON OPERATOR FOR THE KICKED TOP

We turn now to apply the method where \hat{U} is approximated by a finite dimensional matrix to mixed systems (where in some parts of phase space the motion is chaotic and in other parts it is regular). The Ruelle-Pollicott theorem does not apply to such systems. It will be demonstrated, however, that the Ruelle-Pollicott resonances are meaningful and describe the decay of correlations in the chaotic component of mixed systems for a time that may be very long. Asymptotically power-law decay takes place, due to sticking to regular islands in phase space.

In this section the kicked top [3], that was defined by (10) and (11), will be analyzed. It is a summary of results that were presented in [10] (see also [17] and [18]). The phase space is shown in Fig. 2.

A natural basis for this problem is of spherical harmonics

$$Y_{lm}(\theta, \varphi) = (-1)^m \sqrt{\frac{2l+1}{4\pi} \frac{(l-m)!}{(l+m)!}} P_l^m(\cos\theta) e^{im\varphi}. \quad (60)$$

Alternatively one can choose a basis of real functions with $e^{im\varphi}$ replaced by $\sin m\varphi$ and $\cos m\varphi$, resulting in a real matrix for \hat{U} . It is naturally ordered by increased resolution. A truncation at $l = l_{max}$ is introduced. The dimension of the truncated matrix $\hat{U}^{(N)}$, approximating \hat{U} is $N = (l_{max} + 1)^2$. As l_{max} is increased the eigenvalues of $\hat{U}^{(N)}$ converge to values inside the unit circle in the complex plane, as can be seen from Table I.

$l_{max} = 30$	$l_{max} = 40$	$l_{max} = 50$	$l_{max} = 60$
0.7700	0.7688	0.7523	0.7696
0.3075	0.3429	0.3523	0.3550
$\pm i 0.5740$	$\pm i 0.6140$	$\pm i 0.6211$	$\pm i 0.6199$
-0.3170	-0.3348	-0.3444	-0.3388
$\pm i 0.6003$	$\pm i 0.6272$	$\pm i 0.6283$	$\pm i 0.6243$
-0.0042	-0.0002	-0.0100	-0.0058
$\pm i 0.7161$	$\pm i 0.7133$	$\pm i 0.6930$	$\pm i 0.7080$
-0.7025	-0.7228	-0.7155	-0.7165
0.6544	0.6230	0.6495	0.6480
...	-0.5619	-0.5753	-0.5667

TABLE I. Eigenvalues of $\hat{U}^{(N)}$ for $\tau = 10.2$ truncated at $l_{max} = 30, 40, 50$ and 60 (Table I of [10]).

The corresponding eigenfunctions are presented in Fig. 4.

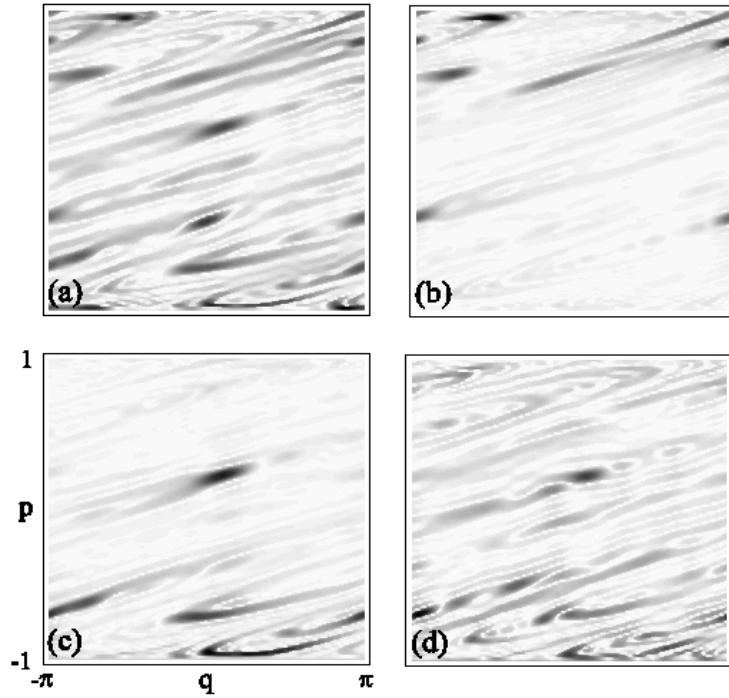


FIG. 4. The eigenfunctions corresponding to the eigenvalues 0.7696 (a), $-0.3388 \pm i0.6243$ (b), $-0.0058 \pm i0.7080$ (c), 0.6480 (d) of $\hat{U}^{(N)}$ for $\tau = 10.2$, and $l_{\max} = 60$ (Fig. 4 of [10]).

Dark-shaded regions in phase space indicate large amplitudes of the eigenfunctions. In Figs. 5 (a) and (b)

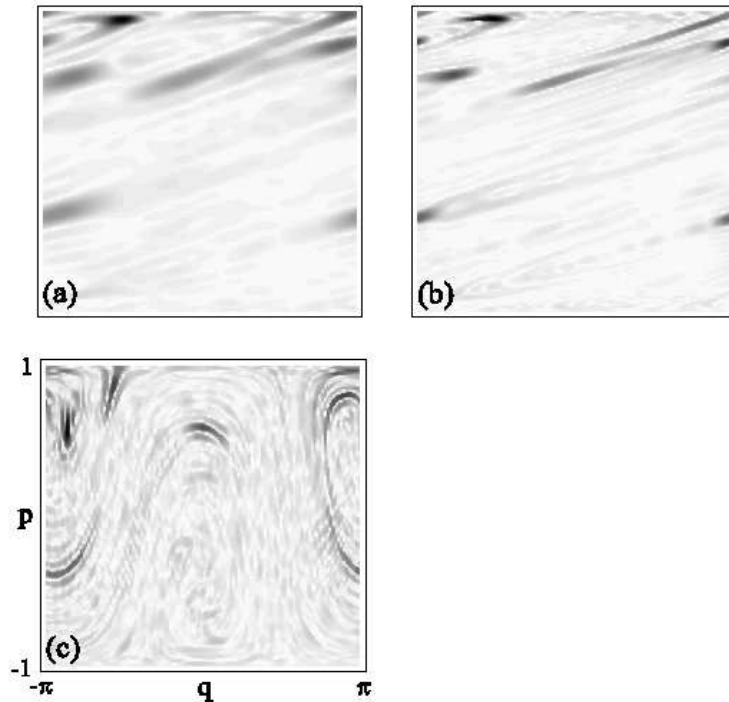


FIG. 5. As phase-space resolution increases from $l_{\max} = 30$ (a) to $l_{\max} = 60$ (b), the eigenfunction of $\hat{U}^{(N)}$ for the eigenvalue $-0.3388 \pm i0.6243$ (for $\tau = 10.2$) gains new structures on finer scales. The corresponding eigenfunction (c) of $\hat{U}^{T(N)}$ (resolution $l_{\max} = 60$) is localized at the same periodic orbit as the eigenfunction (b) but with stable and unstable manifolds interchanged. See also figure 6(a) for the periodic orbits, figure 6(b) for the unstable and figure 6(c) for the stable manifolds (Fig. 5 of [10]).

it is demonstrated that as l_{max} increases finer details of the eigenfunctions are revealed. This is a result of increased resolution. Comparison with Fig. 6 (b)

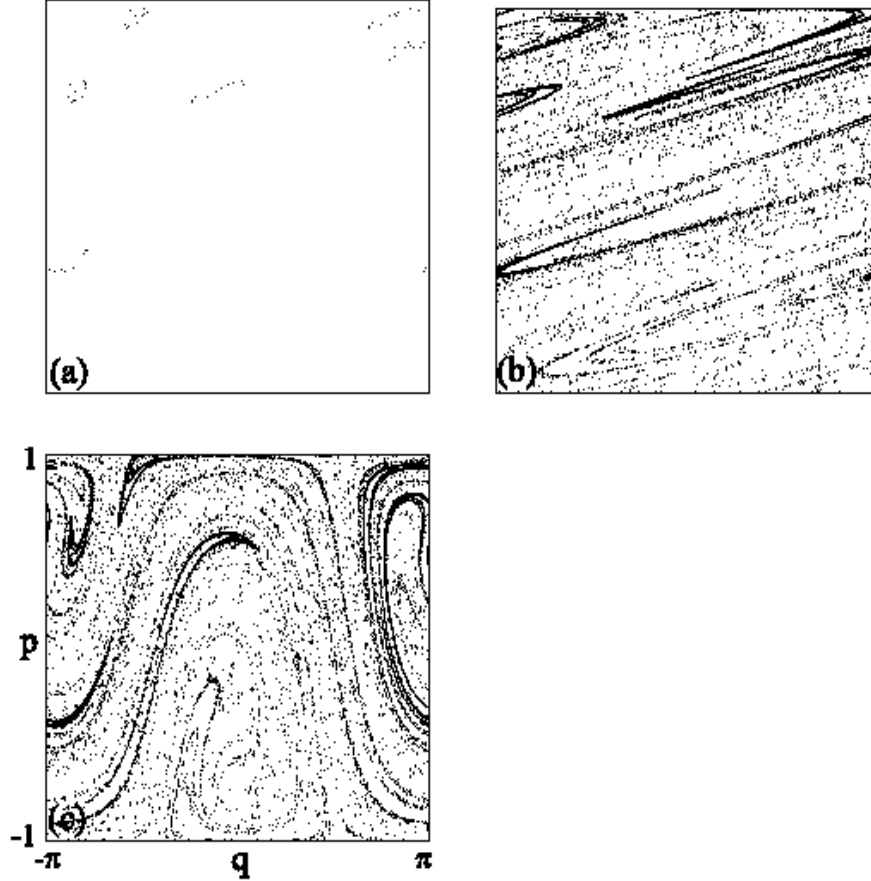


FIG. 6. (a): The 12 orbits of primitive length 6 that can be identified for the resonances $0.3550 \pm i0.6199$ and $-0.3388 \pm i0.6243$ related to the eigenfunction shown in figures 4(b) and 5(b). The unstable manifolds of these orbits are shown in (b), and the stable manifolds in (c) (Fig. 6 of [10]).

demonstrates that the eigenfunctions are large and tend to be uniform on the unstable manifold. In Fig. 7

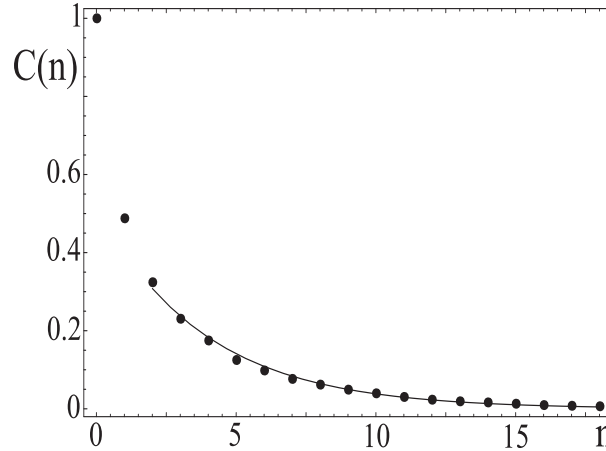


FIG. 7. The decay of $C(n)$ (dots) with $\rho(0)$ corresponding to the eigenfunction shown in figure 4(b) (also 5(b)). The numerical fit (line) yields a decay factor 0.7706 (compared to $|z_i^{(N)}| \approx 0.7103$). (Fig. 7 of [10]).

the density-density correlation function (proportional to (28)) is plotted. It is demonstrated that also here the

Ruelle-Pollicott resonances describe the decay of correlations for a very long time.

The behavior of the eigenfunctions localized in regular regions and the corresponding eigenvalues is very different. Eigenfunctions that are localized in islands of regular motion presented in Fig. 2 (a) are depicted in Fig. 8.

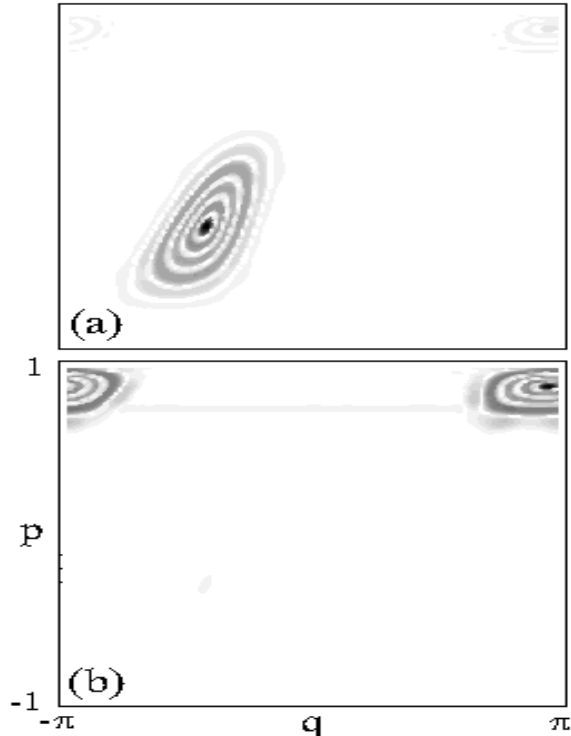


FIG. 8. Eigenfunctions of $\hat{U}^{(N)}$ with $l_{\max} = 60$ that are localized on elliptic islands shown in Fig. 2 (a) for the weakly chaotic case $\tau = 2.1$. The corresponding eigenvalues 0.999976 (a) and 0.999974 (b) are almost at unity (Fig. 3 of [10]).

The eigenfunctions follow elliptic orbits inside the regular island and therefore do not involve the resolution of very fine structures. The corresponding eigenvalues approach the unit circle in the complex plane as l_{\max} increases.

It is instructive to examine the evolution operator \hat{U}^{-1} corresponding to the inverse map \mathbf{F}^{-1} . Unitarity implies

$$\hat{U}^{-1} = \hat{U}^\dagger. \quad (61)$$

A basis can be chosen so that \hat{U} is real and $\hat{U}^\dagger = \hat{U}^T$, where T denotes transpose. The eigenvalues of \hat{U}^T are equal to the ones of \hat{U} . Introducing the truncation one finds

$$\hat{U}^{T(N)} = \hat{U}^{(N)T}, \quad (62)$$

where $\hat{U}^{T(N)}$ is the truncated \hat{U}^T and $\hat{U}^{(N)T}$ is the transpose of $\hat{U}^{(N)}$, the truncated \hat{U} . The eigenfunctions of $\hat{U}^{T(N)}$ are localized on the unstable manifold of \mathbf{F}^{-1} , that is the stable manifold of \mathbf{F} , as is clearly demonstrated comparing Fig. 5 (c) with Fig. 6 (c). By eigenfunctions we meant so far the right eigenfunctions. The left eigenfunctions of \hat{U} (and $\hat{U}^{(N)}$) are the right eigenfunctions of \hat{U}^T (and $\hat{U}^{T(N)}$).

The main results that were obtained for the kicked top are:

1. As N or l_{\max} increases the eigenvalues of $\hat{U}^{(N)}$, corresponding to eigenfunctions localized in the chaotic component of phase space, converge to values inside the unit circle. Unlike the case of the baker map, the eigenvalues $z_i^{(N)}$ depend on N and $\lim_{N \rightarrow \infty} z_i^{(N)} = z_i$ with $|z_i| < 1$, except the unit eigenvalue corresponding to the equilibrium density.
2. These eigenvalues determine the decay of correlations in the chaotic component of phase space.
3. In the chaotic component of phase space the right eigenfunctions of the truncated Frobenius-Perron operator $\hat{U}^{(N)}$ are localized on the unstable manifold of \mathbf{F} , and tend to be uniform along this manifold. The left eigenfunctions are localized on the stable manifold. These manifolds are not as simple as for the baker map.

4. The eigenvalues of $\hat{U}^{(N)}$ corresponding to eigenfunctions localized in regular regions approach the unit circle as N or l_{max} increases.

V. THE FROBENIUS-PERRON OPERATOR FOR THE KICKED ROTOR

In this section the decay of correlations in time will be studied for the kicked rotor, defined by the Hamiltonian (6), and its dynamics is given by the standard map (8) [1,3,7]. The phase space is presented in Fig. 1. It is a mixed system (where in some regions of phase space the motion is chaotic and in other regions it is regular). In this section we summarize results that were presented in [19] (see also [20], [23] and [16]).

For sufficiently large values of the stochasticity parameter K (that takes a typical value), the spread of angular momentum is diffusive, to a good approximation, namely

$$\langle (J_n - J_0)^2 \rangle \approx 2Dn, \quad (63)$$

for large n . The average is over the initial points and is denoted by $\langle \dots \rangle$. A very crude way to get this result is to iterate (8) n times to obtain

$$J_n - J_0 = K \sum_{i=1}^n \sin \theta_i, \quad (64)$$

then squaring and averaging with the assumption of absence of angular correlations

$$\langle \sin \theta_i \sin \theta_j \rangle = \frac{1}{2} \delta_{ij}, \quad (65)$$

one obtains (63) with $D = \frac{1}{4}K^2$. A more careful calculation, that takes some of the angular correlations into account results in [24]

$$D(K) = \frac{K^2}{4} \left(1 - 2J_2(K) + \dots \right). \quad (66)$$

It is actually an expansion in powers of $1/\sqrt{K}$. Because of the mixed nature of phase space it is expected that diffusion may not take place asymptotically in time [25]. Moreover, there are values of K (near integer multiples of 2π) where acceleration in momentum is found for some initial conditions, resulting in $\langle (J_n - J_0)^2 \rangle \sim n^2$. In what follows the Frobenius-Perron operator will be used to study whether correlations in angular momentum decay as expected for a true diffusion process, described in the Introduction (see (16)-(23)). We will analyze also the decay of angular correlations.

The Frobenius-Perron operator, corresponding to the map (8) on the torus

$$(0 \leq J < 2\pi s) \quad (67)$$

$$(0 \leq \theta < 2\pi),$$

where s is integer, will be studied. For the usual kicked rotor $s \rightarrow \infty$. Noise is added to the standard map by the addition of a random variable ξ_n with variance σ^2 on the right hand side of the equation for θ_{n+1} in (8) following [24]. The noise leads to truncation of the Frobenius-Perron operator. The natural basis for the analysis is

$$\langle J\theta | km \rangle = \frac{1}{\sqrt{2\pi}} \frac{1}{\sqrt{2\pi s}} \exp(im\theta) \exp\left(i \frac{kJ}{s}\right). \quad (68)$$

where k and m are integers. Note that the functions $\langle J\theta | k, m = 0 \rangle$ form the basis of eigenstates of the diffusion operator in the angular momentum J . In this basis, in presence of noise, the Frobenius-Perron operator is

$$\langle km | \hat{U}^{(\sigma)} | k' m' \rangle = J_{m-m'} \left(\frac{k'K}{s} \right) \exp\left(-\frac{\sigma^2}{2} m^2\right) \delta_{k-k', ms}. \quad (69)$$

For $\sigma \neq 0$ the operator is not unitary. The effective truncation is $m < 1/\sigma$, $|k - k'| < s/\sigma$, $|m - m'| < k'K/s$. The $\sigma \rightarrow 0$ limit, corresponding to the $N \rightarrow \infty$ limit of the previous sections, will be taken in the end of calculation. The analysis will be performed for

$$\begin{aligned}
s &\gg 1 \\
K &\gg 1 \\
\frac{kK}{s} &\ll 1
\end{aligned} \tag{70}$$

and the limit $\sigma \rightarrow 0$ will be taken in the end of the calculation.

The Ruelle resonances are identified from the matrix elements of the resolvent (31). It is useful to define a variant of the resolvent

$$\hat{R}'(z) = \sum_{j=0}^{\infty} \hat{U}^j z^j = \frac{1}{1 - z\hat{U}} \tag{71}$$

that is related to $\hat{R}(z)$ via

$$\frac{1}{z} \hat{R}'\left(\frac{1}{z}\right) = \hat{R}(z). \tag{72}$$

Also the matrix elements of \hat{R} and \hat{R}' satisfy (72). Let

$$R_{12} = \langle k_1 m_1 | \hat{R}(z) | k_2 m_2 \rangle \tag{73}$$

and

$$R'_{12} = \langle k_1 m_1 | \hat{R}'(z) | k_2 m_2 \rangle \tag{74}$$

be the matrix elements of \hat{R} and \hat{R}' respectively. Therefore a singularity of R_{12} at z_c implies a singularity of R'_{12} at $1/z_c$ and vice versa. The series (31) for $\hat{R}(z)$ converge for $|z| > 1$ while the series (71) for $\hat{R}'(z)$ converge for $|z| < 1$. Therefore the Ruelle-Pollicott resonance (located inside) that is closest to the unit circle corresponds to the singularity of R'_{12} that is closest to the unit circle (located outside). This singularity is the radius of convergence of the series

$$R'_{12} = \sum_{j=0}^{\infty} a_j z^j, \tag{75}$$

where

$$a_j = \langle k_1 m_1 | \hat{U}^j | k_2 m_2 \rangle. \tag{76}$$

According to the Cauchy-Hadamard theorem (see [26]) the inverse of the radius of convergence is given by

$$r^{-1} = \lim_{j \rightarrow \infty} \sup \sqrt[j]{|a_j|}. \tag{77}$$

and asymptotically

$$|a_j| \sim \frac{\text{const.}}{r^j}. \tag{78}$$

Since the radius of convergence is the singularity of $R'_{12}(z)$ that is the closest to the unit circle it satisfies $r = 1/z_c$ and $\sqrt[j]{a_j} \rightarrow z_c$ in the limit $j \rightarrow \infty$ (at least for some subsequence of $\{j\}$).

The limit of the series (76) was found in the leading order in perturbation theory in the small parameters implied by (70). The calculation can be performed separately for the various values of k , resulting in

$$z_k = \exp\left(-\frac{k^2 K^2}{4s^2} \left(1 - 2J_2(K)e^{-\sigma^2}\right)\right), \tag{79}$$

corresponding to diffusion modes in presence of noise. Taking the limit $\sigma \rightarrow 0$ one finds

$$z_k = e^{-k^2 D(K)/s^2} \tag{80}$$

where $D(K)$ is given by (66). This relaxation is similar to the one that is found for usual diffusion (see (16-23)). The relaxation rates are

$$\gamma_k = \frac{k^2}{s^2} D(K), \quad (81)$$

that correspond to (20). These describe the decay of correlations in angular momentum J . The equilibrium density corresponds to z_0 . Exploring the subspace involving $|k = 0, m\rangle$, one finds that the Ruelle-Pollicott resonances, corresponding to the slowest mode of the relaxation of correlations in angle, take four values

$$\pm \tilde{z}, \quad \pm i\tilde{z} \quad (82)$$

with

$$\tilde{z} = \sqrt{|J_{2m^*}(m^*K)| \exp(-\sigma^2 m^{*2}/2)}. \quad (83)$$

Taking the limit $\sigma \rightarrow 0$ one finds

$$\tilde{z} = \sqrt{|J_{2m^*}(m^*K)|}, \quad (84)$$

where m^* is the integer m that maximizes $|J_{2m}(mK)|$ for a given value of K . A similar result was found in [16] by a variational approach. The corresponding relaxation rate is

$$\tilde{\gamma} = \ln \tilde{z}. \quad (85)$$

In order to test the analytical results, the correlation function of the form (29)

$$C_{fg}(n) = \langle f | \hat{U}^n | g \rangle, \quad (86)$$

where f and g are taken to be basis states of (68), was computed numerically. The results are plotted in Fig. 9.

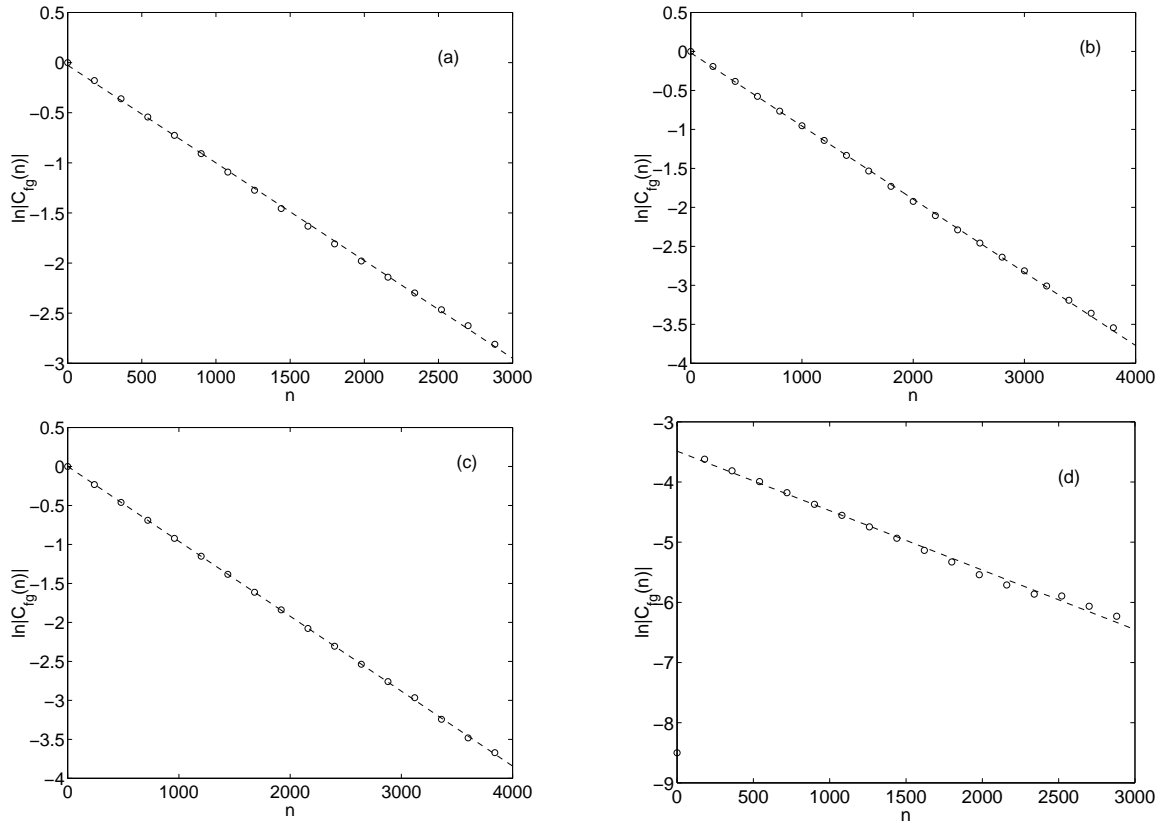


FIG. 9. The function $C_{fg}(n)$ for: (a) $K = 20$; (b) $K = 30$; (c) $K = 40$; (d) $K = 27$, for various functions f and g and for various values of s (Fig. 1 of [19]).

Clear exponential decay is found. From the slopes, the relaxation rates γ_k are obtained for the various modes, k . The values of D implied by γ_k are calculated from (81) and compared to the ones obtained from (66) in Fig. 10.

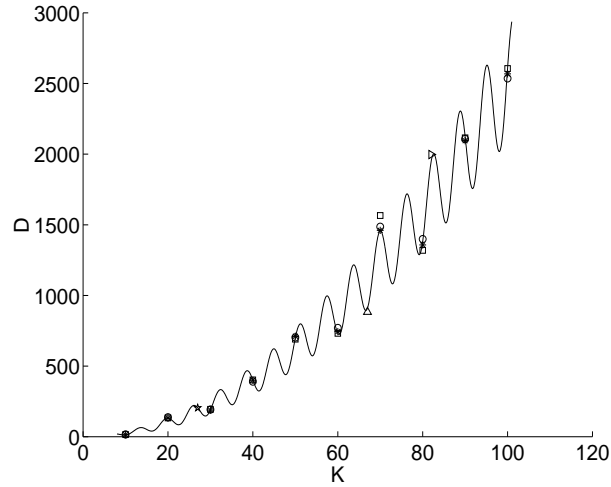


FIG. 10. The diffusion coefficient D for $K \geq 10$ as found from plots like the ones presented in Fig. 9. Various symbols represent results found for different modes k while the solid line represents the analytical value (66) (Fig. 2 of [19]).

Good agreement was found. In Figs. 9 and 10 large values of the stochasticity parameter, $K \geq 10$, were used. In this regime the regular regions are extremely small (they are invisible in Fig. 1), therefore the theory presented in this review is expected to work very well, as is indeed found in Fig. 10. In Fig. 11 the correlation function (86) is presented for $K \leq 20$.

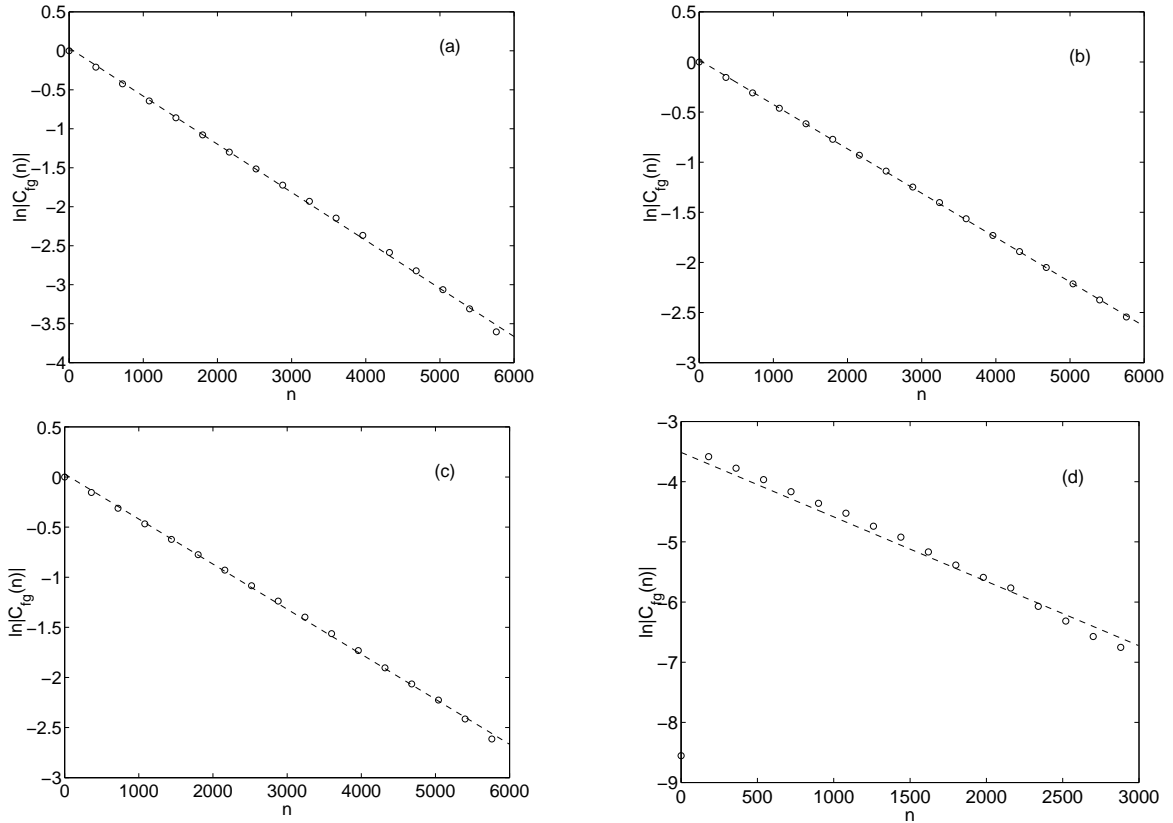


FIG. 11. The function $C_{fg}(n)$ for: (a) $K = 7$; (b) $K = 8$; (c) $K = 3$; (d) $K = 17$, for various functions f and g and for various values of s (Fig. 3 of [19]).

From these results the relaxation rates γ_k were calculated. The resulting values of the diffusion coefficient obtained from (81) are compared to the ones found from (66) in Fig. 12, for $K \leq 20$. Here, in contrast to the regime of large K presented in Fig. 10, appreciable deviations are found.

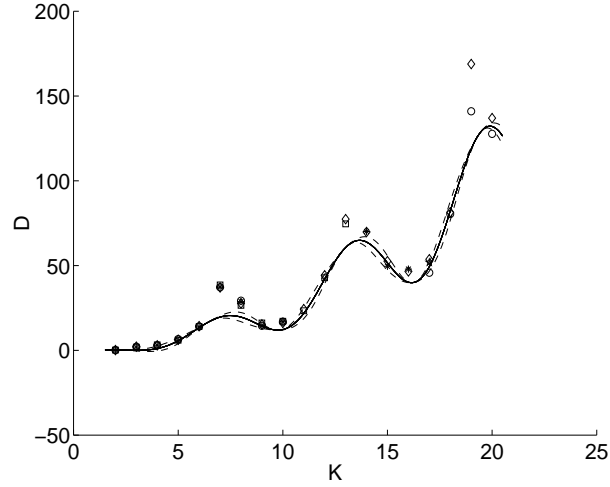


FIG. 12. The diffusion coefficient D for $K \leq 20$ as found from plots like the ones presented in Fig. 11. Various symbols represent results found for different modes k while the solid line represents the analytical value (66). The dashed line represents the approximate error, resulting of the truncation of the perturbation theory expansion. The values of D obtained by direct simulation of propagation of trajectories are marked by diamonds (Fig. 4 of [19]).

These are related to sticking to regular structures, that is not taken into account in the theory presented in this review. To test the decay of correlations in the angle variable, the correlation function (86) was computed for $|f\rangle$ and $|g\rangle$ that are basis states of the form $|k = 0, m\rangle$, and some of the results are presented in Fig. 13.

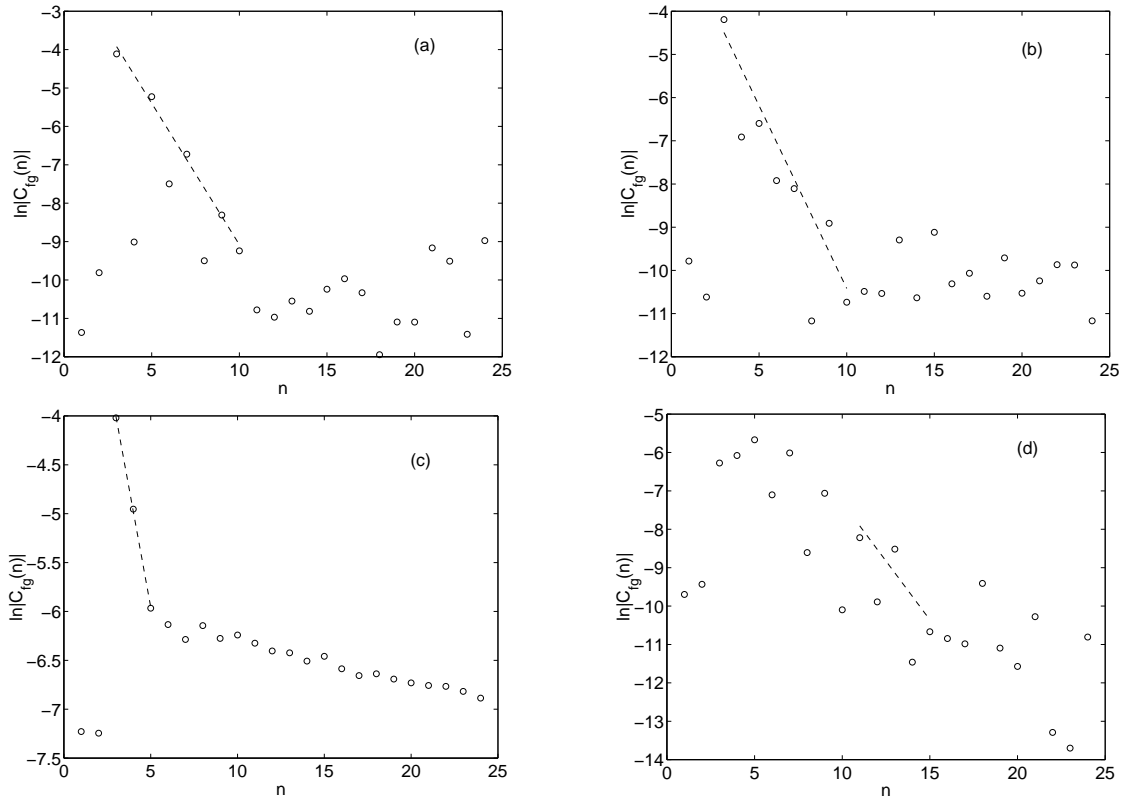


FIG. 13. The function $C_{fg}(n)$ for $s = 1$ with $|f\rangle = |01\rangle$, $|g\rangle = |02\rangle$ and (a) $K = 16.3$; (b) $K = 19.5$; (c) $K = 12$; (d) $K = 16$. The dashed line represents the best fit to the data (Fig. 5 of [19]).

The relaxation is very fast, therefore it is very difficult to estimate numerically the relaxation rate. The numerical results are compared to the analytical prediction (85) in Fig. 14.

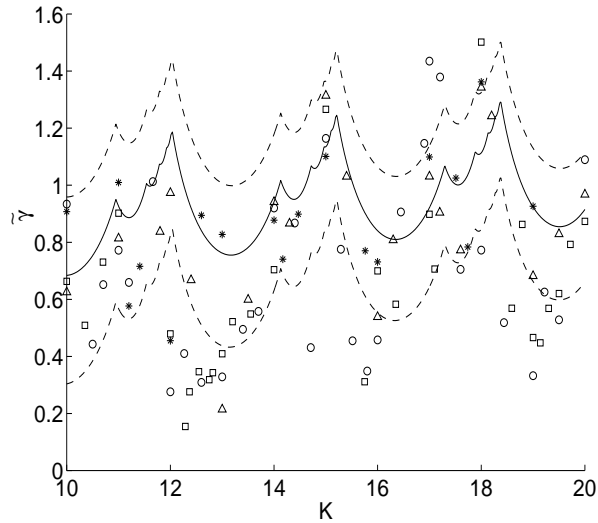


FIG. 14. The fast relaxation rates $\tilde{\gamma}$ as found from plots like Fig. 13 for various functions f and g with $k = 0$, marked by various symbols. The analytical value (85) is represented by a solid line while the dashed lines denote the analytically estimated error, resulting of the truncation of the perturbation theory expansion (Fig. 7 of [19]).

The analytical formula provides a reasonable estimate of the relaxation rate and of its dependence on the stochasticity parameter K . There are however deviations that are significant. Also here some of the most significant deviations were found to be related to regular structures.

The main results that were obtained for the kicked rotor are:

1. Addition of noise results in the effective truncation of the Frobenius-Perron operator. In the limit of vanishing noise the Ruelle-Pollicott resonances are found. The resonances depend on the noise, and therefore on the truncation, as is the case for the kicked top, and approach limiting values inside the unit circle in the limit of vanishing noise, except the unit eigenvalue corresponding to the equilibrium density.
2. The Ruelle-Pollicott resonances determine the decay of correlations.
3. Deviations from exponential decay of correlations may be found after some time as a result of the existence of regular structures.
4. The following physical picture emerges. First the correlations in the angle variable θ decay. Then the correlations in angular momentum J decay as for a true diffusion process. For finite s a uniform equilibrium density is reached. For $s = \infty$, after the decay of the angular correlations, diffusive spreading takes place.
5. At some time, that is increasing with the stochasticity parameter K , sticking to regular structures becomes important, and the picture based on Ruelle-Pollicott resonances and exponential decay of correlations, breaks down.

VI. SUMMARY

It was demonstrated that Ruelle-Pollicott resonances are relevant even when the conditions for the Ruelle-Pollicott theorem do not hold. A method for the calculation of these resonances by a finite truncation of the Frobenius-Perron operator was presented. The relation between the resonances and the decay of correlations was established under these conditions. For mixed systems (as well as for other nonhyperbolic systems) the picture breaks down after some time, that may be very long, as a result of sticking to regular structures.

In order to evaluate the relevance of the Ruelle-Pollicott resonance picture for realistic systems it is instructive to introduce several time scales:

1. If γ_1 is the slowest decay rate (corresponding to the resonance that is closest to the unit circle), $t_{chaos} = 1/\gamma_1$ is the decay time of correlations and the relaxation time to the invariant density.
2. The time scale when sticking to regular structures becomes important will be denoted by t^* .
3. In presence of external noise correlations are destroyed on the time scale $t_c \sim 1/\sigma^2$, where σ^2 is the variance of the noise.

In order to observe the exponential decay of correlations it is required that

$$t_{chaos} \ll t_c, t^*. \quad (87)$$

Destruction of sticking to regular structures requires $t_c < t^*$. In the regime

$$t_{chaos} \ll t_c < t^* \quad (88)$$

the decay of correlations is expected to be similar to the one of hyperbolic systems and one should be able to explore it in the framework of the method that was outlined in the present review. Application of the method to specific examples is of great interest.

ACKNOWLEDGMENTS

It is our great pleasure to thank Fritz Haake for many illuminating discussions during the preparation of the lectures and of the review, for the files of the figures from [10] and for the permission to use them. Part of the review is based on work in collaboration with Oded Agam and Maxim Khodas, that is acknowledged with great pleasure. We would like to thank Christopher Manderfeld and Joachim Weber for useful discussions and communications. SF thanks Andreas Buchleitner for the hospitality at the Max Planck Institute for the Physics of Complex Systems in Dresden, where the lectures were prepared. This research was supported in part by the US-Israel Binational Science Foundation (BSF), by the Minerva Center of Nonlinear Physics of Complex Systems, by the Max Planck Institute for the Physics of Complex Systems in Dresden, and by the fund for Promotion of Research at the Technion.

- [1] E. Ott, *Chaos in Dynamical Systems*, (Cambridge University Press, Cambridge, 1997).
- [2] V.I. Arnold and A. Avez, *Ergodic Problems of Classical Mechanics*, (Addison-Wesley NY, 1989).
- [3] F. Haake, *Quantum Signatures of Chaos*, (Springer-Verlag, Berlin, 1991).
- [4] B.G Schuster, *Deterministic Chaos, An Introduction*, (Physik-Verlag, Weinheim, 1984).
- [5] P. Gaspard, *Chaos, Scattering and Statistical Mechanics*, (Cambridge Press, Cambridge 1998).
- [6] J.R. Dorfman, *An Introduction to Chaos in Non-Equilibrium Statistical Mechanics*, (Cambridge Press, Cambridge 1999).
- [7] A.J. Lichtenberg and M.A. Lieberman, *Regular and Stochastic Motion* (Springer, NY 1983).
- [8] F. L. Moore, J. C. Robinson, C. F. Bharucha, Bala Sundaram, and M. G. Raizen, Phys. Rev. Lett. **75**, 4598 (1995); C. F. Bharucha, J. C. Robinson, F. L. Moore, Qian Niu, Bala Sundaram, and M. G. Raizen, Phys. Rev. **E 60**, 3881 (1999).
- [9] B. Fischer, A. Rosen, A. Bekker and S. Fishman, Phys. Rev. **E**, R4694 (2000).
- [10] **J. Weber, F. Haake, P.A. Braun, C. Manderfeld and P. Šeba, J. Phys. **A 34**, 7195 (2001).
- [11] M. V. Berry, in *New trends in Nuclear Collective Dynamics*, eds: Y. Abe, H. Horiuchi, K. Matsuyanagi, Springer proceedings in Physics. vol **58** pp183-186 (1992).
- [12] D. Ruelle, Phys. Rev. Lett. **56**, 405 (1986).
- [13] **H.H. Hasegawa and W.C. Saphir, Phys. Rev. **A 46**, 7401 (1992).
- [14] S. Fishman, in *Supersymmetry and Trace Formulae, Chaos and Disorder*, edited by I.V. Lerner, J.P. Keating, D.E. Khmelnitskii (Kluwer Academic / Plenum Publishers, New York, 1999).
- [15] A. Jordan and M. Srednicki, The approach to Ergodicity in the Quantum Baker's Map, nlin.CD/0108024 (2001), This paper contains also some results on the classical baker's map, that are relevant for the present review.
- [16] G. Blum and O. Agam, Phys. Rev. **E 62**, 1977 (2000).
- [17] J. Weber, F. Haake and P. Šeba, Phys. Rev. Lett. **85**, 3620 (2000).
- [18] C. Manderfeld, J. Weber and F. Haake, J. Phys. **A 34**, 9893 (2001).
- [19] **M. Khodas, S. Fishman and O. Agam, Phys. Rev. **E 62**, 4769 (2000).

- [20] M. Khodas and S. Fishman, Phys. Rev. Lett. **84**, 2837 (2000); Erratum **84**, 5918 (2000).
- [21] We thank E. Bogomolny, M. Saraceno, M. Srednicki and A. Jordan for illuminating comments.
- [22] M. Basilio de Matos and A.M. Ozorio de Almeida, Ann. Phys. (N.Y.) **237**, 46 (1995).
- [23] R. Balescu, *Statistical Dynamics, Matter out of Equilibrium*, (Imperial College Press ,Singapore, 1983).
- [24] A.B. Rechester and R.B. White, Phys. Rev. Lett. **44**, 1586 (1980); A.B. Rechester M.N. Rosenbluth and R.B. White, Phys. Rev. **A 23**, 2664 (1981); E. Doron and S. Fishman, Phys. Rev. **A 37**, 2144 (1988).
- [25] B. Sundaram and G.M. Zaslavsky, Phys. Rev. **E 59**, 7231 (1999); G.M. Zaslavsky, M. Edelman and B.A. Niyazov, Chaos **7**, 159 (1997).
- [26] K. Knopp, *Infinite Sequences and Series*, (Dover publ. NY, 1956).

Most of the results presented in the review can be found in references marked by **